

## Biomimetic chitosan-mediated synthesis in heterogeneous phase of bulk and mesoporous silica nanoparticles

Victoria Puchol, Jamal El Haskouri,\* Julio Latorre, Carmen Guillem, Aurelio Beltrán, Daniel Beltrán and Pedro Amorós\*

### Electronic Supplementary Information

#### Details on the preparative conditions

All the dynamic experiments were performed at 25°C by circulating (0.05 mL/s) dilute pre-hydrolyzed TEOS solutions (from 0.001 M to 0.1 M) on chitosan flakes confined in a small zone of the reactor (see Figure S1). The alkoxide pre-hydrolysis was performed during 30 minutes in a buffered (Na-phosphate) aqueous solution or using simulated sea water. In all cases, the working pH value was close to 7. In a typical synthesis leading to Sample 2, 5.57 mL of TEOS were added to 250 mL of a simulated sea water solution (0.5 M), and the mixture was maintained under vigorous stirring during 30 min. to start the alkoxide hydrolysis. The resulting partially hydrolyzed solution was circulated to the reactor where a chitosan flake (0.012 mg) was included. Static experiments (without stirring) were carried out exactly under the same conditions.

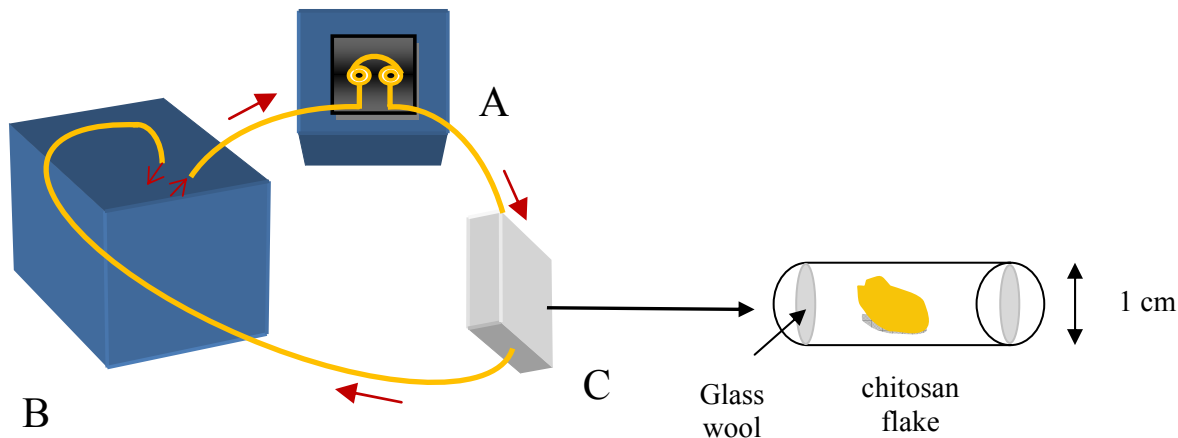


**Figure S1.** Scheme of the dynamic reactor used. A = Peristaltic pump. B = Thermostatic bath. C = Reactor containing the chitosan flake.

In the synthesis of MCM-41 and SBA-15-like silicas, both in the case of dynamic and static conditions (see Table 1 in the manuscript), the SDA (“structural directing agent”, namely CTABr

-cetyltrimethyl ammonium bromide- or Pluronic P123 -Poly(ethylene glycol)-*block*-poly(propylene glycol)-*block*-poly(ethylene glycol)-, respectively) was directly added to the pre-hydrolyzed TEOS solution. In typical static syntheses: (1) The alkoxide pre-hydrolysis was performed during 30 min. in simulated sea water (100 mL), (2) a solution of the SDA agent in 150mL of sea water was then added to the pre-hydrolyzed TEOS solution, and the chitosan was immediately incorporated to the resulting mixture, (3) the recovered white mesostructured solids were washed, dried and calcined at temperatures in the 400-550°C range. The Si : SDA molar ratios used here are similar to those previously reported in the bibliography for the synthesis of MCM-41 (Si : 0.25 CTABr) and SBA-15 (Si : 0.01 P123) mesoporous silicas.<sup>1,2</sup>

In order to test the ability of simple amines to promote the polymerization and aggregation of silica under biomimetic conditions, we carried out additional experiments by using additives as ammonia, dodecylamine (DDA) or octadecylamine (ODA). In all three cases we used similar concentration conditions ( $[Si] = 0.1 \text{ M}$ , and a very low nitrogen concentration ( $1.07 \cdot 10^{-9} \text{ NH}_3/\text{DDA/ODA} : 1 \text{ Si}$ )), which in turn result in concentration of amine groups similar to those occurring at the chitosan surface. In the case of  $\text{NH}_3$ , a weak turbidity was detected in the solution after 5-7 days. When DDA or ODA were added, precipitation was appreciable after 24-48 hours. In all cases, the final solids are constituted by aggregation of silica nanoparticles. No mesoporous materials were obtained even by increasing the DDA or ODA concentrations (1 Si : 0.26 DDA/ODA).

### Chitosan as solid additive

According to the bibliography data,<sup>3</sup> the chitosan flakes should be considered as an insoluble additive at the circum-neutral pH conditions used in our experiments. In any case, given that this is a key point concerning our preparative approach as a whole, we present here a clear probe of the chitosan insolubility under the reaction conditions.

Thus, we have recorded FTIR spectra of the liquid reaction media in contact with chitosan flakes after long reaction times under the pH and T conditions used in our biomimetic syntheses. Fourier transform infrared spectroscopy (FTIR) was carried out by using a Thermo Electron Corporation Diamond system ( $200\text{--}30000 \text{ cm}^{-1}$ ). The analyses were performed in the transmission mode in the  $500\text{--}4000 \text{ cm}^{-1}$  range, with a resolution of  $4 \text{ cm}^{-1}$  and an accumulation of 32 scans.

Shown in Figure S2 are the FTIR spectra of solutions containing chitosan flakes in sea water at  $t = 0$  (red curve) and  $t = 3$  days (blue curve) compared with a spectrum of the same solution acidified with acetic acid ( $\text{pH} = 1.6$ ;  $t = 0$ ; green curve). The represented curves correspond to the registered spectra after background subtraction (due to the sea water absorption). The spectra in Figure S2 clearly confirm that, under the preparative conditions used, chitosan

remains insoluble and, consequently, the whole system whose chemistry we are dealing with must be considered heterogeneous. Moreover, no swelling of the flakes is observed.

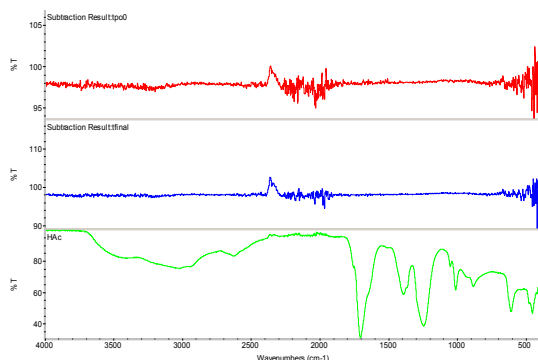


**Figure S2.** FTIR spectra of liquid reaction media at different times and pH.

### EDX analysis

All the prepared samples actually correspond to basically pure silica materials. In practice, all the final solids are amine-free materials, in accordance with the above mentioned chitosan flakes insolubility. This specific fact has been confirmed both by IR spectroscopy and thermal analysis of the samples. Moreover, irrespective of the reaction medium (Na-phosphate buffered solutions or simulated sea water), the final materials only incorporate small amounts of cations and/or anions. Shown in Figure S3 is a representative EDX analysis corresponding to Sample 2 (1Na : 51Si; 1Mg : 44Si; 1Cl : 28Si).

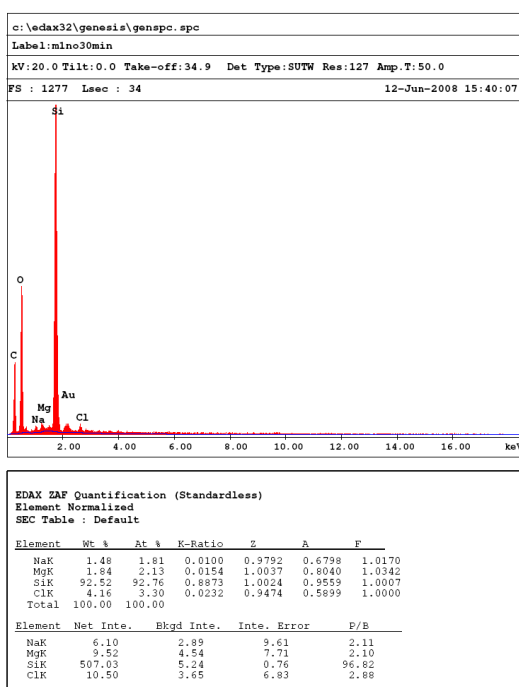


**Figure S3.** EDX analysis of Sample 2.

### N<sub>2</sub> adsorption-desorption isotherms and particle size modulation in bulk materials

Shown in Figure S4 is a N<sub>2</sub> adsorption-desorption isotherm that can be considered as representative of the behaviour of bulk nanoparticulated biosilicas. In the absence of SDA molecules, we can observe only a single and sharp adsorption step at relatively high partial pressure. This step can be related to capillary condensation inside the large inter-particle voids generated as the nucleation, growth and aggregation of the nanoparticles proceeds. In practice, the formation of a continuous network based on soldered nanoparticles generates a disordered system of large void-pores (ranging from large-meso to macropores) accounting for the observed textural porosity. The non-ordered nature of this large pore system is consistent with a formation mechanism implying collision and aggregation of primary nanoparticles, in which does not participate any SDA agent able to transfer a certain organization.

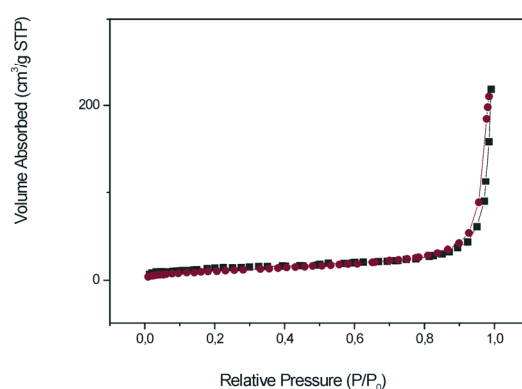


**Figure S4.** N<sub>2</sub> adsorption desorption isotherm of Sample 4 (BET surface area = 53 m<sup>2</sup>/g; BJH pore volume = 0.25 cm<sup>3</sup>/g; BJH pore size = 18.2 nm).

As can be noted (see Figure 1 and Table 1 of the manuscript), the particle size is slightly larger when Na-phosphate is used to control the pH of the reaction medium. It has been stated that the concentration of phosphate in solution is a factor promoting the increasing of the particle size because it favours the size of the polyamine aggregates in solution.<sup>4</sup> However, in the present case, the presence of chitosan as solid flakes (insoluble) allows discarding such a relationship. Instead of this, it seems to be the ionic strength of the medium (provided by the buffer or the simulated sea water) which is responsible for the observed differences, as it was claimed for dendrimer-templated silicas.<sup>5</sup> In practice, when a concentrated Na-phosphate buffer solution (1 M) is used, the reaction proceeds in the presence of a high concentration of relatively small Na<sup>+</sup> cations. These can effectively neutralize the charge of terminal SiO<sup>-</sup> groups, what would result in a concomitant decrease of the inter-particle electrostatic repulsions facilitating the particle growth.

### N<sub>2</sub> adsorption and desorption isotherms and TEM image of Sample 8 (prepared with P123)

Shown in Figures S5 and S6 are the N<sub>2</sub> adsorption and desorption isotherms and a TEM image corresponding to Sample 8, which are commented in the manuscript.

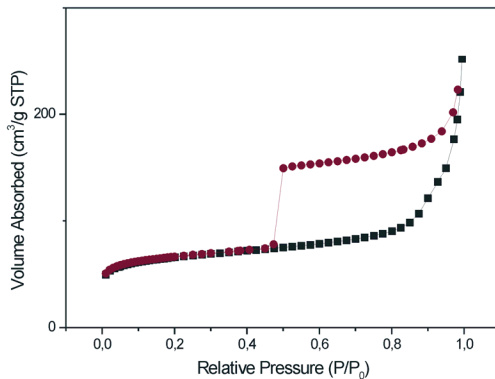


**Figure S5.** N<sub>2</sub> adsorption desorption isotherm of Sample 8 (BET surface area = 174 m<sup>2</sup>/g; BJH pore volume = 0.24 cm<sup>3</sup>/g).

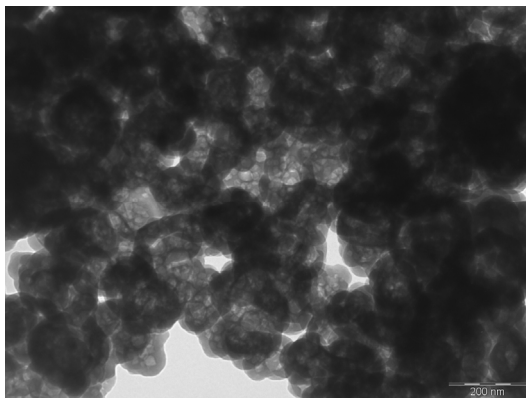


**Figure S6.** TEM image of Sample 8.

### Comment on the disordered nature of the MCM-like biosilicas

In syntheses like those we are dealing with, the high dilution conditions used affect both the inorganic and organic counterparts and also their cooperative self-assembling. Thus, at such high dilutions, the surfactant concentration is clearly lower than that corresponding to its *cmc* value. If so, the surfactant species in solution will be isolated molecules instead of pre-organized micelles. On the other hand, with regard to the inorganic species, we can reasonably expect a relatively high (or at least moderate) polymerization degree of the silica entities because of the circum-neutral pH conditions used.

Self-assembling from building blocks with not properly balanced sizes (large silica oligomers/small surfactant species) hinders their organization in highly symmetric arrays, what leads in practice to hexagonal disordered mesopore systems.

### Suggested role played by chitosan

The real role played by biomimetic additives has raised some controversy.<sup>6</sup> A recent sound study concludes that, in aqueous media, the effect of alcoholic OH-containing additives on the silica polymerization could be considered negligible.<sup>7</sup> However, there is consensus concerning the importance of amine nitrogen functional groups in regulating the amorphous silica production.<sup>8,9</sup> Terminal amine groups could play a bi-functional role, acting as agents promoting both the silica condensation and the particle aggregation processes. Thus, proton-transfer from terminal amines could catalyze TEOS hydrolysis through a SN<sub>2</sub> mechanism, a process that seems to be fast at pH values around the amine pK<sub>a</sub>, where concentrations of the conjugated acid/base species are similar.<sup>10</sup> These optimal conditions happen in our case; the circum-neutral pH conditions, that avoid the chitosan flakes dissolution, warrant the coexistence of surface terminal NH<sub>2</sub> and NH<sub>3</sub><sup>+</sup> groups (insofar as an apparent pK<sub>a</sub> of 6-7 is accepted for chitosan).<sup>3</sup> Then, the well known nucleophilic properties of chitosan (under the working pH conditions)<sup>10,11</sup> could be responsible for promoting the silica polymerization on the flake surface.

On the other hand, the ability of amine containing organic molecules to act as aggregation promoters is well known. In fact, the electrostatic interactions between negatively charged silica species and positively charged amino groups (*f.e.* amino-containing peptides or the own chitosan in solution) have been identified as responsible for silica precipitation in determined cases.<sup>12,13</sup> Here, assuming a 50% of protonated amino groups, we can estimate an inter-NH<sub>3</sub><sup>+</sup> centres average distance of *ca.* 1.2-1.4 nm. The accordingly located electrostatic interactions would help to shorten the distances among silica nanoparticles and would facilitate, therefore, the silica precipitation in the form of clusters constructed by nanoparticle aggregation. Once attained a certain critical size, such clusters might leave the flake surface (where more silica-amino interactions would proceed), and the silicate oligomers might be further polymerized in solution. Moreover, taking into account the extremely low proportion of amine groups (at the chitosan surface)/Si (see Table 1), in the range 4·10<sup>-8</sup> – 5·10<sup>-6</sup>, it is reasonable to assume that the clusters of nanoparticles might be desorbed of the chitosan surface in order to allow the complete processing of the silica species in solution.

### Bio-inspired syntheses

Contrary of expectations in the case of pure inorganic syntheses time consuming can be an important factor when designing particular bio-inspired preparative strategies. In the case of

diatoms it is usually assumed that the frustules replications imply two differentiated steps: the silicic acid accumulation and the silica deposition. Then, although some diatoms are able to produce a silica valve (deposition step) in a relatively short time (from some minutes to hours), this occurs after very large times of Si-species accumulation. In fact, regardless the specific diatom species or intracellular pool sizes, a concentration of soluble silica monomers or olygomers above saturation is required for the formation of the silica valve. Hence, without subtle biological systems favouring the concentration and stabilization of small silica olygomers (as occurs in diatoms), the experiments carried out under biomimetic conditions usually lead to silica deposition, but they require long reaction times.

In our case, we have performed different bio-inspired synthesis experiments by increasing the TEOS or the additive (chitosan) concentrations. In all cases the reaction times have been shortened in a significant way.

In the case of MCM-41-like biosilicas, extremely quick precipitation occurs when the TEOS concentration is increased up to 0.5 M (Sample 9)(Figure S7).



**Figure S7** Immediate precipitation (< 1sec) of a MCM-41-like biosilica.

On the other hand, when the chitosan amount is increased from *ca.* 0.012 g to 1 g (while maintaining a relatively low silica concentration, 0.1 M), the formation of silica nanoparticles (Sample 10) is accelerated in a significant way (from several days, as occurs for Samples 1 and 3, to only a few hours). Figure S8 shows the evolution of a typical experiment at t = 0, 5 and 15 hours.

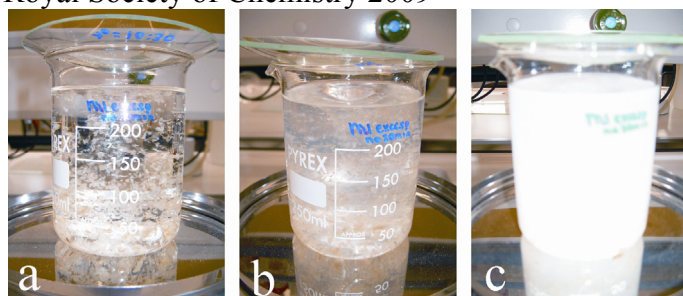


**Figure S8** Experiment carried out with a large excess of chitosan at different reaction times for Sample 10. (a)  $t = 0$  h. (b)  $t = 5$  h. (c)  $t = 15$  h.

## References

- 1 C. T. Kresge, M. E. Leonowicz, W. J. Roth, J. C. Vartuli, J. S. Beck, *Nature*, 1992, **359**, 710.
- 2 S.-S. Kim, T. R. Pauly, T. J. Pinnavaia, *Chem. Commun.*, 2000, 1661.
- 3 G. F. Payne, S. R. Raghavan, *Soft Matter.*, 2007, **3**, 521.
- 4 E. Brunner, K. Lutz, M. Sumper, *Phys. Chem. Chem. Phys.*, 2004, **6**, 854.
- 5 M. R. Knecht, S. L. Sewell, D. W. Wright, *Langmuir*, 2005, **21**, 2058.
- 6 S. V. Patwardhan, S. J. Clarson, C. C. Perry, *Chem. Commun.*, 2005, 1113, and references therein.
- 7 G. E. Tilburey, S. V. Patwardhan, J. Huang, D. L. Kaplan, C. C. Perry, *J. Phys. Chem. B*, 2007, **111**, 4630.
- 8 D. Belton, G. Paine, S. V. Patwardhan, C. C. Perry, *J. Mater. Chem.*, 2004, **14**, 2231.
- 9 T. Coradin, C. Roux, J. Livage, *J. Mater. Chem.*, 2002, **12**, 1242.
- 10 K. M. Delak, N. Sahai, *J. Phys. Chem. B*, 2006, **110**, 17819.
- 11 B. Krajewska, *Enzyme Microb. Technol.*, 2004, **35**, 126.
- 12 T. Coradin, O. Durupthy, J. Livage, *Langmuir*, 2002, **18**, 2331.
- 13 J. S. Chang, Z. L. Kong, D. F. Hwang, K. L. B. Chang, *Chem. Mater.*, 2006, **18**, 702.